Journal of the Mechanical Behavior of Biomedical Materials 78 (2018) 420–426

Contents lists available at ScienceDirect

Journal of the Mechanical Behavior of Biomedical Materials

journal homepage: www.elsevier.com/locate/jmbbm

Characterization of a new decellularized bovine pericardial biological mesh: Structural and mechanical properties

Alessandra Bielli[a,1], Roberta Bernardini[b,e,1], Dimitrios Varvaras[c,1], Piero Rossi[c], Giancarlo Di Blasi[d], Giuseppe Petrella[c], Oreste Claudio Buonomo[c], Maurizio Mattei[a,e,*,1], Augusto Orlandi[a,1]

[a] Institute of Anatomic Pathology, Department of Biomedicine and Prevention, Tor Vergata University, Rome, Italy
[b] Centro Servizi Interdipartimentale – STA, University of Rome "Tor Vergata", Rome, Italy
[c] Department of Experimental Medicine and Surgery, University of Rome "Tor Vergata", Italy
[d] Brachi Testing Services Srl, Prato, Italy
[e] Dept. of Biology, University of Rome "Tor Vergata", Rome, Italy

ARTICLE INFO

Keywords:
Biomesh
Bovine pericardium
Tissue decellularization

ABSTRACT

Implants made from naturally-derived biomaterials, also called biological meshes or biomeshes, typically derive from decellularized extracellular matrix of either animal or human tissue. Biomeshes have many biomedical applications such as ligament repair, bone and cartilage regeneration and soft tissue replacement. Bovine collagen is one of the most widely used and abundantly available xenogenic materials. In particular, bovine pericardium is widely used as extracellular matrix bioprosthetic tissue. The efficiency of a pericardial mesh to function as scaffold depends on the quality of the decellularization protocol used. Moreover, the biomesh mechanical features are critical for a successful surgical repair process, as they must reproduce the biological properties of the autologous tissue. Different methods of physical, chemical, or enzymatic decellularization exist, but no one has proved to be ideal. Therefore, in the present study, we developed a novel decellularization protocol for a bovine pericardium-derived biomesh. We characterized the biomesh obtained by comparing some ultrastructural, physical and mechanical features to a reference commercial biomesh. Quantification revealed that our novel decellularization process removed about 90% of the native pericardial DNA. Microscopic and ultrastructural analysis documented the maintenance of the physiological structure of the pericardial collagen. Moreover, mechanical tests showed that both the extension and resilience of the new biomesh were statistically higher than the commercial control ones. The results presented in this study demonstrate that our protocol is promising in preparing high quality bovine pericardial biomeshes, encouraging further studies to validate its use in tissue engineering and regenerative medicine protocols.

1. Introduction

Tissue engineering is a multidisciplinary field that includes the production of scaffolds used as supporting materials to restore, maintain or even improve tissue anatomy and function (Zonari et al., 2012). Membranes typically derive from either animal tissue or synthetic polymers. Biological meshes, also called "biomeshes", are constituted of pure collagen matrix derived from human, porcine, or bovine tissue through a decellularization process. Grafted biomeshes act as a regenerative framework that supports remodeling and new collagen deposition. Once implanted, the ideal biomesh is gradually and fully integrated into the host tissue, promoting cellular and vascular regeneration and *de novo* formation of tissues similar to the normal ones (Pascual et al., 2012).

Biomedical research and tissue engineering scientists have identified the essential prerequisites of an ideal biomesh (Wang et al., 2006): a biodegradable material with satisfactory biomechanical behavior, efficient host tissue incorporation, high cell compatibility, and a low inflammatory response (Scheidbach et al., 2004). The characteristics of each graft are unique and depend on the tissue source and the specific protocol used for decellularization (Keane et al., 2012). Usually tissues are processed to remove all components, cells and debris, that can cause an inflammatory immunoreaction following implantation, while retaining as much as possible the three dimensional ultrastructure and

* Correspondence to: Centro Servizi Interdipartimentale – STA University of Rome "Tor Vergata", Via Montpellier 1, 00133 Rome, Italy.
E-mail address: mattei@uniroma2.it (M. Mattei).
[1] These authors contributed equally to this work.

https://doi.org/10.1016/j.jmbbm.2017.12.003
Received 31 July 2017; Received in revised form 21 November 2017; Accepted 1 December 2017
Available online 05 December 2017
1751-6161/

composition of the native extracellular matrix (ECM) (Schmidt and Baier, 2000). In addition, biomaterials used in reconstructive surgery should be highly compatible with the function of the native tissue, providing mechanical properties matching the tissue to be replaced (Rohrnbauer and Mazza, 2013, 2014).

At present, biomeshes are mainly obtained from five different types of tissue: bovine pericardium, human cadaveric dermis, porcine small intestine submucosa, porcine dermal collagen, and bovine dermal collagen (Bellows et al., 2013). Over the last decade, bovine pericardium-derived biomeshes have been evaluated in numerous studies. In particular, bovine pericardium was used for repairing abdominal defects in a rat model (Zuki et al., 2007), in replacement of aortic valve in the ovary model (Amaral et al., 2010), in the reconstruction of the tendons in the chicken (Sungur et al., 2006), and abdominal surgery for the reinforcement/anastomosis healing (Testini et al., 2014). Several methods of decellularization have been introduced to obtain an appropriate biomesh (Booth et al., 2002; Courtman et al., 1994; Kasimir et al., 2003). Decellularization methods of bovine pericardium include mechanical, chemical, detergent, and enzymatic techniques, or a combination thereof. Each of them has different effects upon both the resulting biologic scaffold and the associated host remodeling response and outcome. However, the combination of the different methods can minimize adverse effects on the remaining matrix constituents of the decellularized tissue (Crapo et al., 2011; Keane et al., 2015).

The aim of the present study was to develop a novel protocol of decellularization to obtain a bovine pericardium biomesh with superior characteristics compared to commercially available ones. Therefore, Assut Europe S.p.A. modified a well-established protocol, developed, on a new substrate (bovine pericardium) produced for human application. To characterize our non-cross-linked biomesh derived from bovine pericardial tissue, called Bioripar®, we analyzed its structural and mechanical properties and compared them to a commercial biomesh, named Tutomesh®, RTI Surgical Inc, USA.

2. Materials and methods

2.1. Tissue preparation

For preparation of Bioripar® mesh (Bioripar®, ASSUT Europe, Rome, Italy), bovine pericardial membranes were obtained from a local slaughterhouse. We selected cattle of the same age from the slaughterhouse to get pericardia with a thickness comprised between 0.4 and 0.7 mm. Immediately after slaughter, the tissue was rinsed with distilled water to remove blood and body fluids and dissected to remove the external fat, then transported in a saline solution (0,9% w/v NaCl). Warm ischemic time was less than 2 h.

2.2. Decellularization protocol

The effective removal of antigenic epitopes associated with cell membranes and intracellular components of tissues and organs is necessary to minimize or avoid an adverse immunologic response by allogeneic and xenogeneic recipients of the scaffold material (Badylak and Gilbert, 2008). To remove all cellular material without adversely affecting the composition, mechanical integrity, and biological activity of the scaffold ECM, four stages of processing of the bovine pericardium were performed:

1. Hypertonic solution treatment: tissues were immersed into hypertonic saline solution 7,5% (w/v) for 20 min to destroy cells, and alternately into purified water to wash residues away; this step was repeated three times at room temperature (RT = 25 °C).
2. Treatments with alkaline and neutralizing solutions: tissues were soaked into phosphate-borate buffer (0.2 M, pH 9.0) for 10 min at RT, to remove most of the antigenicity due to the presence of proteins and proteoglycans of cell membranes. Subsequently, tissues were immersed in a 1 M sodium hydroxide solution (pH > 13.0) for one hour and half, then soaked in a 5% boric acid solution (pH 9) for one hour at RT. Since sodium hydroxide and boric acid solutions digest unnecessary protein and proteoglycan residues, they help with antigen elimination. In addition, this stage completely inactivates most of pathogens.
3. Stabilization: after a thorough washing in purified water, tissues were soaked into a bacteriostatic solution containing propylene glycol 30% in ethanol (w/v) for 15 min at RT.
4. Sterilization: after being cut to size, membranes were packaged in double aluminum pouches and sterilized by γ-irradiation with a 21 kGy (Singh et al., 2016). Membranes were then kept at room temperature until use.

The here presented decellularization protocol differs from the one for the Tutomesh® for the following major points: a) it does not require oxidation with H2O2; b) NaOH is used in alkaline treatment and c) acetone is used in the dehydration stage. This last stage is not present in our protocol.

2.3. DNA isolation and quantification

Residual cell material from the decellularized tissue was evaluated using a low-density microarray (GeneTop Meat V kit, LifeLineLab, Italy) for species identification, able to detect DNA traces ($\geq$ 0.001%). To perform a low-density microarray, genomic DNA was purified from 200 mg of the decellularized tissue (three different pieces for each brand) using the QIAamp® DNA Mini kit (Qiagen, Italy), according to the manufacturer's protocol. DNA concentration was calculated by spectrometric measurements and adjusted to a concentration of 20 ng/μL. Samples of 2.5 μL of the purified DNA were analyzed according to manufacturer's instructions and the presence of a specific spot for the bovine zoological species evaluated. All measurements were performed in triplicate.

2.4. Mechanical characterization

The mechanical properties were characterized by two mechanical tests, namely uniaxial tensile test and burst test. These two tests assess the mesh stiffness by using a load applied in-plane (tensile stiffness) and a load applied perpendicular to the mesh (distension) (Deeken et al., 2011).

To compare mechanical properties of Bioripar® to those of a reference commercial biomesh (Tutomesh®), three pieces of each were used. Membranes were extracted from the sterile package and re-hydrated with saline for at least ten minutes, then they were cut into four scaffolds for the tensile test and one for the bursting strength test. Mechanical tests were carried out in an ISO 17025 Accredited Laboratory (Brachi Testing Services Srl, Prato Italy).

Four specimens of each biomesh were prepared as a dogbone shape of 1 cm wide and 6 cm long, with a narrowed central region approximately 0.4 cm wide and 1.5 cm long (Fig. 1A) using a template sharp. The main thickness of each sample was measured in six different points by using a micrometer. To carry the experiments out under conditions as similar as possible to the *in vivo* ones, all samples were drawn from the central part of the biomesh. Specimens were orientated in different directions to simulate *in vivo* applications. This test allows to determine the ultimate tensile stress and strength and to evaluate the anisotropic characteristics of the biomeshes. Each specimen had one extremity clamped onto a grip and tension was tested by means of a constant strain rate until mesh failure. Specimens were subjected to uniaxial tension at a rate of 300 mm/min crosshead spread by dynamometer (Constant-Rate-of-Extending machine, Hounsfield HS10) following the Grab Method (EN ISO 13934-1 EN ISO 13934-2 with different settings). Stress-strain curves were obtained by dividing the recorded load by the specimen cross-sectional area against nominal strain. Tensile stress was

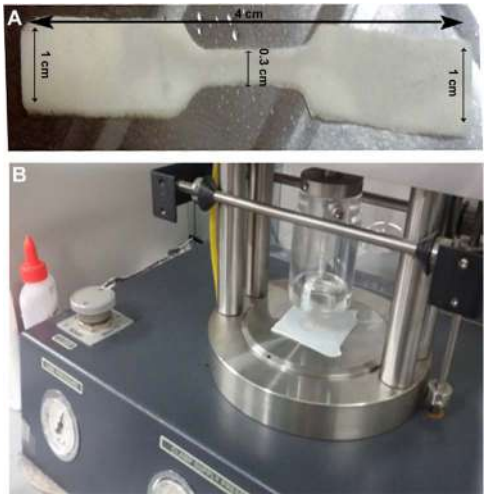

Fig. 1. (A) Picture shows the Uni-axial tensile testing apparatus: a dogbone shaped specimen was placed in a pair of grips which were separated by controlling the rate change in grip separation or specimen strain. A constant force was applied to evaluate the ultimate tensile stress and strength until rupture. (B) Picture shows the Ball burst testing apparatus: the maximum force (bursting force) and the bursting index were calculated as the ratio between the bursting force and the mesh density, letting possible the evaluation of the mesh global mechanical response.

calculated by dividing the load (force) that the specimen sustained (N) during the tensile test by the cross-sectional area (mm^2) of the specimen to yield tensile stress megapascals (MPa) units. The cross-sectional area (mm^2) of the central region of the specimen was calculated by multiplying the width of the central region (0.4 cm) by the scaffold thickness.

The second mechanical test, the ball burst test, was carried out according to EN ISO 13938/1. The Burst Tester (Messmer Buchel M425) was used to measure the bursting strength of biomesh samples subjected to an increasing hydrostatic pressure. Three specimens per biomesh (approximately 6 × 6 cm) were used. Each one was fixed on the top of an extensible membrane by a locking ring (Fig. 1B). Pressure was applied to a circular region of each specimen via an elastic diaphragm. Increasing pressure was applied by a fluid to the lower face of the membrane to cause the deformation of membranes and specimens, since when the pressure was applied, the specimen deformed together with the diaphragm. The bursting strength corresponded to the maximum pressure hold by the specimen before failure.

2.5. Microscopic and histochemical evaluation

For microscopic examination, samples of bovine pericardium ($n = 3$ native and $n = 3$ decellularized tissues) were fixed in 4% paraformaldehyde solution for 20 min and embedded in paraffin. Serial 4 μm thick sections were deparaffinized, rehydrated and stained with Haematoxylin & Eosin as previously reported (Romaniello et al., 2014). Sections were also stained with Verhoeff-Van Gieson (Romaniello et al., 2014) and Masson's Trichrome Stain (Orlandi et al., 2005) to evaluate the degree of loss or fragmentation of elastic and collagen fibers, respectively.

2.6. Transmission electron microscopy and X-ray microanalysis

Structural and morphological integrity of native and decellularized pericardial samples ($n = 3$ controls and $n = 3$ post-decellularization) were investigated by transmission electron microscopy (TEM), after fixation of small tissue samples in Karnovsky's fixative (2% paraformaldehyde, 2.5% glutaraldehyde in 0.1 M phosphate buffer, pH 7.4) for at least 24 h (Cervelli et al., 2012). Ultrathin sections were counterstained with uranyl acetate and lead citrate, then photographed by a Hitachi 710 transmission electron microscope. To evaluate the composition of extracellular matrix depots, X-ray microanalysis was performed using a NORAN™ System 6 Microanalysis System (Thermo Scientific Inc, MA, USA) connected to the TEM microscope.

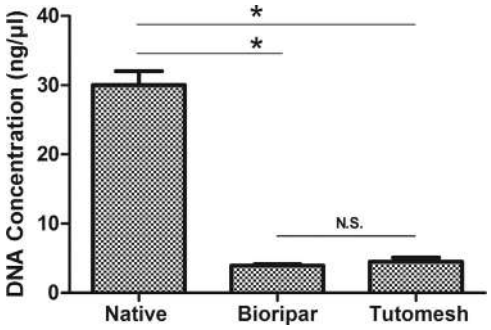

Fig. 2. The graph shows the Mean ± SD of DNA concentration measured in three different biomeshes. Genomic DNA was isolated from 200 mg of $n = 3$ biomesh samples and native bovine pericardium. All sample sets were analyzed in triplicate on the same day. *$p < 0.05$ *versus* native bovine pericardium; N.S. *versus* Tutomesh® (Student's *t*-test).

2.7. Statistical analysis

Data are reported as the mean ± SD. Comparisons between two groups were performed by Student's *t*-test. For analysis of three or more groups of univariate data, single-factor analysis of variation was used. Differences were considered statistically significant when $p < 0.05$.

3. Results

3.1. DNA content

To verify proper DNA removal by our decellularization method, we performed a low-density microarray analysis. As reported in Fig. 2, we documented that after decellularization, Bioripar® biomesh contains ten-fold less DNA than the native bovine pericardium ($p < 0.05$), with a concentration comparable to those of commercial Tutomesh®.

3.2. Decellularization did not modify the characteristics of collagen

Microscopic evaluation confirmed the absence of nuclei after the decellularization process (nuclei counting Mean ± SD: native tissue: 120 ± 33; decellularized tissue: 0 ± 0; $p < 0.0001$). As shown in Fig. 3, the decellularization process did not significantly alter the structure of collagen and elastic fibers, with the organization of collagen fibers being similar to the native bovine pericardium (panel A shows the native pericardium, panel D shows it after decellularization). Moreover, the analysis of histochemical stainings by Masson's Trichrome and Verhoeff-Van Gieson confirmed the maintenance of the morphological appearance of both collagen and elastic fibers (Fig. 3, Panel B, E, C and F, respectively).

3.3. Decellularization did not alter ultrastructural characteristics of collagen fibers

TEM confirmed the efficacy of the decellularization process and the absence of alteration of collagen fibers of bovine pericardium after the process (Fig. 4E and F). Ultrastructural analysis showed that extracellular matrix structure was well preserved as shown in Fig. 4. In particular, the density, consistency and the periodic banding pattern of collagen fibers were almost normal, with a regular distribution of collagen fibers and transverse banding, maintained in decellularized pericardium around at 0.4–0.5 μm. In some randomly selected areas of decellularized pericardium, X-ray microanalysis highlighted the presence of small carbon particles accumulation, featuring residual cell remnants (Fig. 4G).

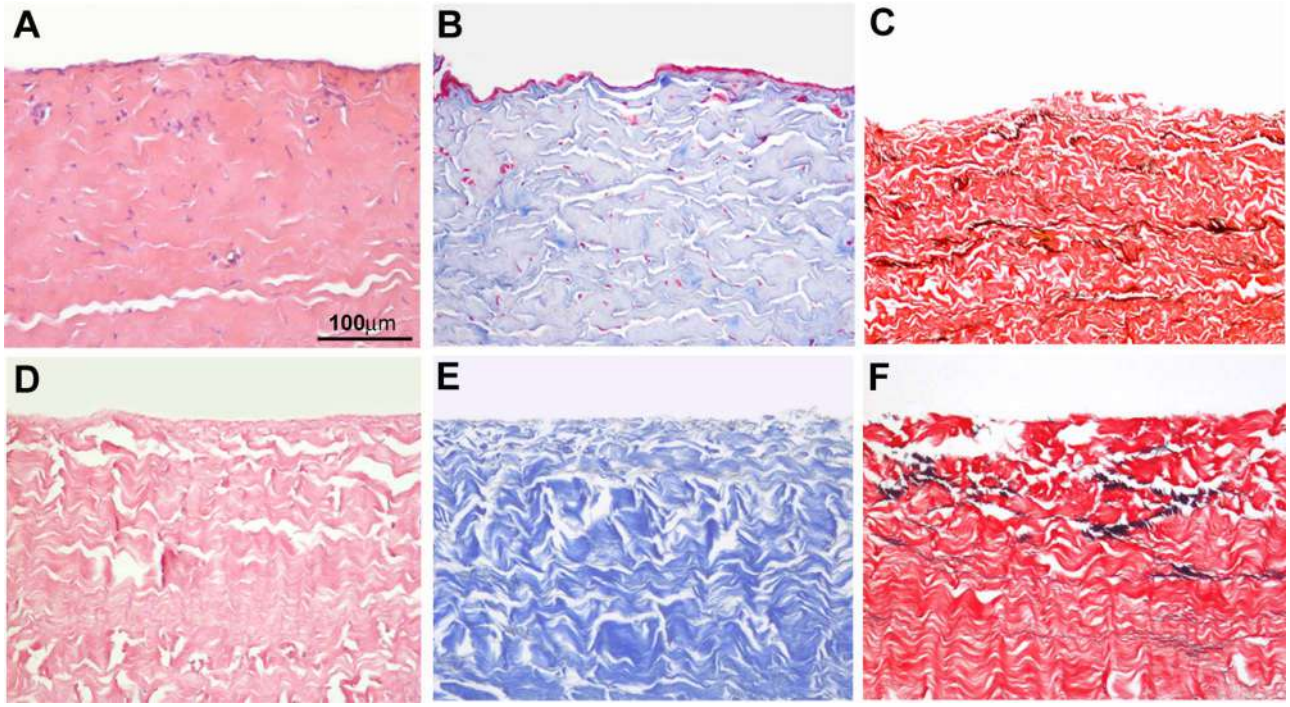

Fig. 3. Representative pictures of three different histological staining show the microscopic aspect of bovine pericardium before and after decellularization. Haematoxylin & Eosin stain of native pericardium bovine sections showed the presence of numerous cell nuclei (A) and their absence after decellularization (D). Masson trichrome staining showed blue-stained collagen tissue and red-stained cells in native collagen (B) and the maintenance of physiological collagen tissue composition with absence of cellular nuclei after decellularization process (E). Verhoeff-Van Gieson staining showed the maintenance of the structure of elastic fibers (black) and of the collagen tissue (red) of bovine pericardium in native conditions (C) and after decellularization (F). Original magnification, 200×.

3.4. Mechanical properties

The evaluation of mechanical properties revealed that Bioripar® specimens were able to hold statistically higher tensile stress than Tutomesh® biomesh ($p < 0.05$, Table 1). Moreover, in the bursting strength test, Bioripar® specimens filled the bell without outburst, whereas Tutomesh® biomesh bursted (Fig. 5, Table 2).

4. Discussion

The knowledge of the structural and mechanical characteristics of engineered biomaterials is crucial in the design and optimization of new biomeshes before their use in the clinical setting. Ideally, an implant should provide mechanical properties matching those of the tissue to be substituted and, also, promote cell proliferation (Badylak and Gilbert, 2008). In the tissue-engineering field, the main purpose for using new biomaterials, as biomeshes, is to achieve both tissue repair and regeneration (Bellows et al., 2007). In fact, once implanted, the biomaterial must favour the formation of new blood vessels and new tissue through the stimulation of the synthesis of new extracellular matrix elements. Some studies demonstrated that both degradation of implanted acellular tissue and tissue regeneration depend on the degree of cross-linkage of the structure of biomaterials (Liang et al., 2004). Among animal tissues selected for biomedical applications, bovine pericardium has some particularly favourable features. In fact, two inseparable biologic surfaces are detectable in the bovine pericardium: the fibrous and the serous parietal layers. The fibrous surface is composed of collagen and elastic fibers, while the serous surface is a basement membrane supporting the mesothelial cell monolayer (Liu et al., 2016). The ability to preserve the extracellular matrix structure after decellularization plays a pivotal role to maintain a suitable microenvironment for facilitating cell growth (Brown and Badylak, 2014). Therefore, the use of decellularized bovine pericardium appears particularly suitable for treatment of multiple pathological conditions (Pascual et al., 2012).

Here, we presented a novel decellularization method introducing some modifications to a well-established protocol adopted by a producer of biomeshes, Assut Europe, for clinical application. This protocol aimed to increase the mechanical properties, strength and extension, of pericardium bovine mesh to be used in breast and abdominal reconstruction where these characteristics are crucial.

We investigated the structural and mechanical properties of a new decellularized bovine pericardium biomesh (Bioripar®) in comparison with a commercial one currently available for surgical use. Typical practices in the study of biological tissue consist in the investigation of histological features in comparison with its native state, in order to define its potential application in the biomedical field. Residual toxicity of a scaffold for the presence of DNA fragments and other cellular component is a critical consideration in development of biomaterials for potential clinical applications (Cebotari et al., 2010). In Bioripar® biomesh, the decellularization process was efficacious; its bovine DNA content was ten-fold lower than the native, not decellularized tissue samples. Further, the DNA concentration was not different from the one in the Tutomesh® biomesh, confirming that commercially available biologic meshes contain trace amounts of residual DNA (Derwin et al., 2006; Gilbert et al., 2009; Zheng et al., 2005). Microscopic analysis confirmed the absence of cell nuclei and the presence of only a few remnants as inert carbon particles. In most of the biologic scaffolds recently investigated, residual DNA is typically present as small fragments (Gilbert et al., 2009); however, the possibility that they may play a substantial adverse role in tissue remodeling has not yet described. In fact, despite the presence of small DNA fragments in commercially available biomeshes, their clinical efficacy is reported to be largely positive (Barber et al., 2006; Brigido, 2006; Catena et al., 2005; Coons and Alan Barber, 2006; Harper, 2001; Lee, 2004; Parker et al., 2006; Sclafani et al., 2000; Smart et al., 2007; Ueno et al., 2004). This supports the hypothesis that small DNA fragments do not induce any significant adverse host response.

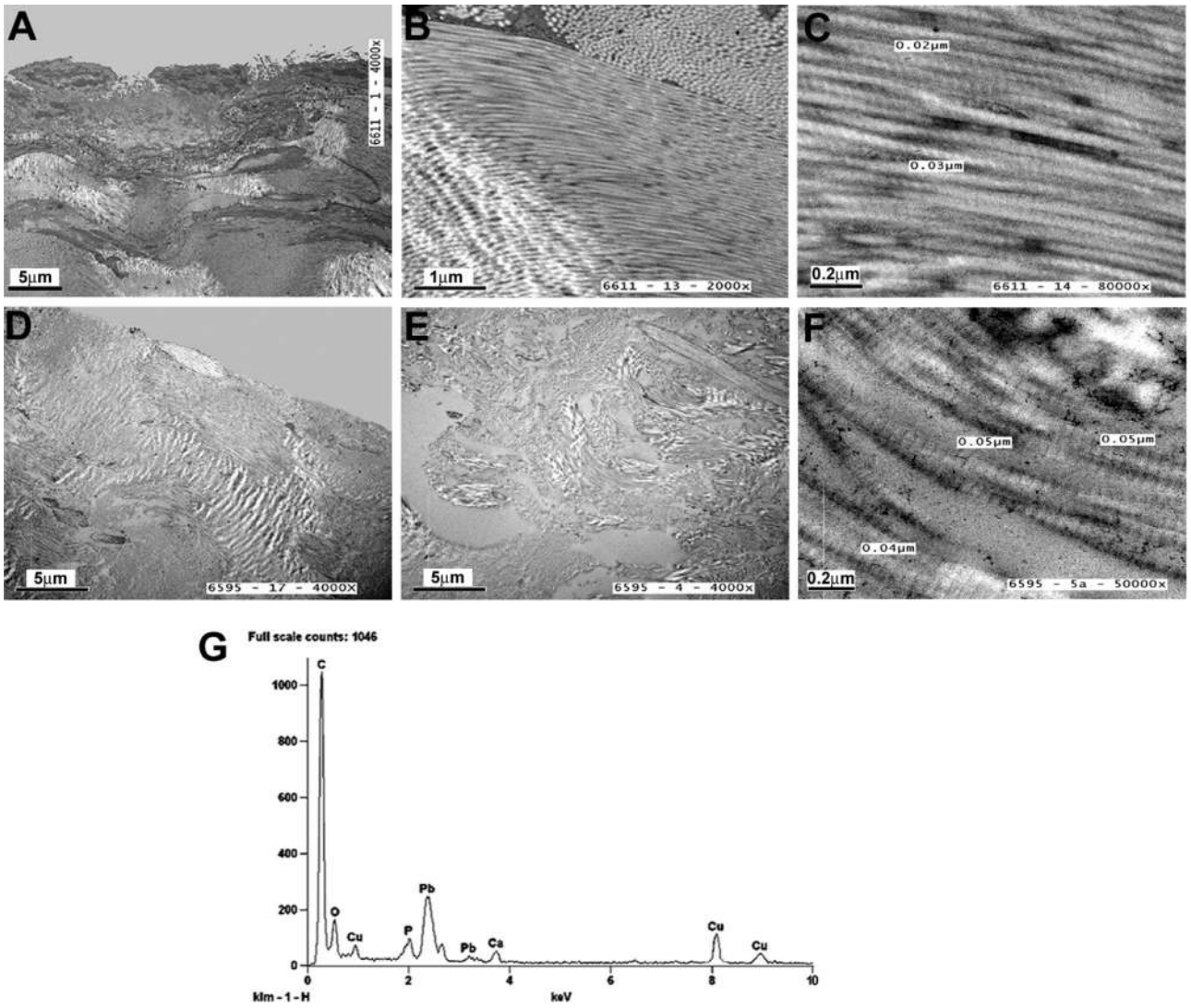

Fig. 4. Representative pictures of Transmission electron microscopy show the ultrastructural aspect of bovine pericardium before and after decellularization treatment. Results showed a normal distribution of collagen fibers and the collagen transverse regular banding with a 0.2–0.3 µm repeat in small samples of native bovine pericardium (A-C). In decellularized pericardium (D-F), the periodic banding pattern of collagen fibers was maintained at 0.4–0.5 µm. (G) X-ray microanalysis of decellularized pericardium showed the presence of cellular carbon residues (C) and lead traces; the latter is contained in the citrate solution for sample preparation. A, D and E original magnification 4000× ; B original magnification 2000× ; C and F original magnification 80,000× .

Table 1
Comparison of thickness and mechanical function of decellularized bovine pericardium.

Mesh	Tissue Thickness (mm)	Tensile Stress (N)	Extension (%)
Bioripar® (n = 4)	0.50 ± 0.04	22.9 ± 6.8*	25.7 ± 6.1
Tutomesh® (n = 5)	0.50 ± 0.05	7.7 ± 3.9	18.5 ± 5.6

n = number of specimens; * = $p < 0.05$.

Our results indicate that the here presented novel decellularization process well preserved the integrity of collagen fibers and mechanical properties of the tissue compared to the native bovine pericardium. In fact, the aim of any decellularization process is to remove cells and their debris preserving the structure and the composition of the native extracellular matrix. These features are of critical importance, since the denaturation of extracellular matrix and collagen could negatively influence the cellular response. In our novel Bioripar® biomesh, both Verhoeff-Van Gieson and Masson's Trichrome stains confirmed the maintenance of collagenous and elastic extracellular matrix components after decellularization. Moreover, results from TEM experiment showed that the decellularized pericardium retained its original morphology as well as a regular distribution of collagen fibers with its characteristic d-banding (around at 0.4–0.5 µm) as in the native pericardium. These observations were corroborated by results from the uniaxial tensile test and the and burst test, demonstrating that Bioripar® biomesh, independently of strip direction, displayed approximately three-fold more tensile strength than Tutomesh®. Moreover, Tutomesh® biomesh failed the test of burst strength, as did Bioripar® one. However, the burst test provides a mechanical response of the mesh, although evaluation of mechanical properties in different directions is not applicable (Todros et al., 2017).

Although the results of the present study appear encouraging, a few limitations are documented. In particular, the complex *in vivo* environment and the different and variable forces applied within the human body may differ and vary in distinct districts with a marked interindividual variability. Moreover, the evaluation of the tensile stress and resistance of the biomesh *in vitro* doesn't fully represent the remodeling process occurring after implantation *in vivo*, when cells populate decellularized extracellular matrix of a scaffold, with consequent *de novo* collagen and protein deposition. For these reasons, *in vivo* studies are currently ongoing on a murine model to understand both the biocompatibility of the mesh, in terms of it integration with

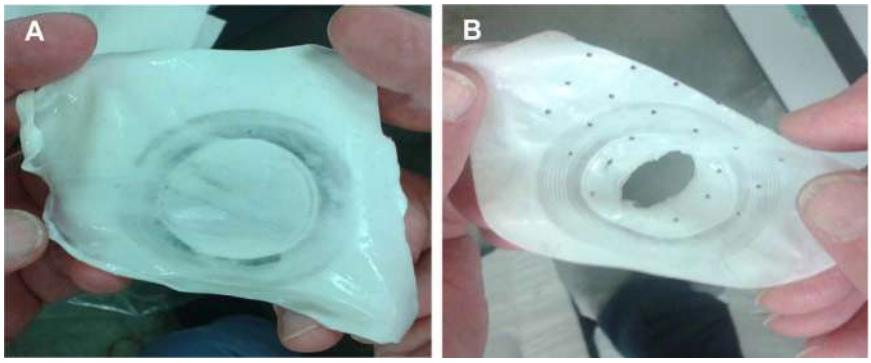

Fig. 5. Pictures show representative biomesh specimens used in the Ball burst test. (A, B) final event of biomeshes undergone to an increasing hydrostatic pressure that causes the deformation or rupture of biomeshes, such as documented for Bioripar® (A) and Tutomesh® (B), respectively.

Table 2
Bursting strength test.

	Bursting strength (KPa)
Bioripar® (n = 3)	560 ± 0*
Tutomesh® (n = 3)	180 ± 19

n = number of specimens for mesh.
* Bioripar® did not burst at the maximal scale value.

surrounding native tissue, and its mechanical properties.

In conclusion, the decellularization process here described allowed us to obtain a new bovine pericardium-derived biomesh, named Bioripar®, with an almost complete decellularization, a good preservation of both extracellular matrix structure as well as of the mechanical properties of native bovine pericardium. These results strongly support the use of Bioripar® in regenerative surgery. Further preclinical studies are needed to validate the efficacy of Bioripar® biomesh as engineered scaffold in several fields, including post-surgical breast reconstruction.

Acknowledgments

This work was partially supported by Assut Europe S.p.A. The authors wish to thank Kalina Gentili, Antonio Volpe and Sabrina Cappelli and Gareth Adam Maglennon for their technical assistance. We thank also Mario Mazzetti for his technical assistance during mechanical tests.

Disclosure statement

The authors declare that they have no conflict of interest.

References

Amaral, J.J., Pomerantzeff, P.M., Casagrande, I.S., Cestari, I.A., Gutierrez, P.S., Stolf, N.G., 2010. Analysis of hemodynamic performance of the bovine pericardium valved conduit, implanted in the aortic position in ovines. Rev. Bras. Cir. Cardiovasc. 25, 543–551.
Badylak, S.F., Gilbert, T.W., 2008. Immune response to biologic scaffold materials. Semin. Immunol. 20, 109–116.
Barber, F.A., Herbert, M.A., Coons, D.A., 2006. Tendon augmentation grafts: biomechanical failure loads and failure patterns. Arthroscopy 22, 534–538.
Bellows, C.F., Albo, D., Berger, D.H., Awad, S.S., 2007. Abdominal wall repair using human acellular dermis. Am. J. Surg. 194, 192–198.
Bellows, C.F., Smith, A., Malsbury, J., Helton, W.S., 2013. Repair of incisional hernias with biological prosthesis: a systematic review of current evidence. Am. J. Surg. 205, 85–101.
Booth, C., Korossis, S.A., Wilcox, H.E., Watterson, K.G., Kearney, J.N., Fisher, J., Ingham, E., 2002. Tissue engineering of cardiac valve prostheses I: development and histological characterization of an acellular porcine scaffold. J. Heart Valve Dis. 11, 457–462.
Brigido, S.A., 2006. The use of an acellular dermal regenerative tissue matrix in the treatment of lower extremity wounds: a prospective 16-week pilot study. Int. Wound J. 3, 181–187.
Brown, B.N., Badylak, S.F., 2014. Extracellular matrix as an inductive scaffold for functional tissue reconstruction. Transl. Res. 163, 268–285.
Catena, F., Ansaloni, L., Leone, A., De Cataldis, A., Gagliardi, S., Gazzotti, F., Peruzzi, S., Agrusti, S., D'Alessandro, L., Taffurelli, M., 2005. Lichtenstein repair of inguinal hernia with Surgisis inguinal hernia matrix soft-tissue graft in immunodepressed patients. Hernia 9, 29–31.
Cebotari, S., Tudorache, I., Jaekel, T., Hilfiker, A., Dorfman, S., Ternes, W., Haverich, A., Lichtenberg, A., 2010. Detergent decellularization of heart valves for tissue engineering: toxicological effects of residual detergents on human endothelial cells. Artif. Organs 34, 206–210.
Cervelli, V., Scioli, M.G., Gentile, P., Doldo, E., Bonanno, E., Spagnoli, L.G., Orlandi, A., 2012. Platelet-rich plasma greatly potentiates insulin-induced adipogenic differentiation of human adipose-derived stem cells through a serine/threonine kinase Akt-dependent mechanism and promotes clinical fat graft maintenance. Stem Cells Transl. Med. 1, 206–220.
Coons, D.A., Alan Barber, F., 2006. Tendon graft substitutes-rotator cuff patches. Sports Med. Arthrosc. 14, 185–190.
Courtman, D.W., Pereira, C.A., Kashef, V., McComb, D., Lee, J.M., Wilson, G.J., 1994. Development of a pericardial acellular matrix biomaterial: biochemical and mechanical effects of cell extraction. J. Biomed. Mater. Res. 28, 655–666.
Crapo, P.M., Gilbert, T.W., Badylak, S.F., 2011. An overview of tissue and whole organ decellularization processes. Biomaterials 32, 3233–3243.
Deeken, C.R., Abdo, M.S., Frisella, M.M., Matthews, B.D., 2011. Physicomechanical evaluation of polypropylene, polyester, and polytetrafluoroethylene meshes for inguinal hernia repair. J. Am. Coll. Surg. 212, 68–79.
Derwin, K.A., Baker, A.R., Spragg, R.K., Leigh, D.R., Iannotti, J.P., 2006. Commercial extracellular matrix scaffolds for rotator cuff tendon repair. Biomech. Biochem. Cell. Prop. J. Bone Jt. Surg. Am. 88, 2665–2672.
Gilbert, T.W., Freund, J.M., Badylak, S.F., 2009. Quantification of DNA in biologic scaffold materials. J. Surg. Res. 152, 135–139.
Harper, C., 2001. Permacol: clinical experience with a new biomaterial. Hosp. Med. 62, 90–95.
Kasimir, M.T., Rieder, E., Seebacher, G., Silberhumer, G., Wolner, E., Weigel, G., Simon, P., 2003. Comparison of different decellularization procedures of porcine heart valves. Int. J. Artif. Organs 26, 421–427.
Keane, T.J., Londono, R., Turner, N.J., Badylak, S.F., 2012. Consequences of ineffective decellularization of biologic scaffolds on the host response. Biomaterials 33, 1771–1781.
Keane, T.J., Swinehart, I.T., Badylak, S.F., 2015. Methods of tissue decellularization used for preparation of biologic scaffolds and in vivo relevance. Methods 84, 25–34.
Lee, M.S., 2004. GraftJacket augmentation of chronic Achilles tendon ruptures. Orthopedics 27, s151–s153.
Liang, H.C., Chang, Y., Hsu, C.K., Lee, M.H., Sung, H.W., 2004. Effects of crosslinking degree of an acellular biological tissue on its tissue regeneration pattern. Biomaterials 25, 3541–3552.
Liu, Z.Z., Wong, M.L., Griffiths, L.G., 2016. Effect of bovine pericardial extracellular matrix scaffold niche on seeded human mesenchymal stem cell function. Sci. Rep. 6, 37089.
Orlandi, A., Ciucci, A., Ferlosio, A., Pellegrino, A., Chiariello, L., Spagnoli, L.G., 2005. Increased expression and activity of matrix metalloproteinases characterize embolic cardiac myxomas. Am. J. Pathol. 166, 1619–1628.
Parker, D.M., Armstrong, P.J., Frizzi, J.D., North Jr., J.H., 2006. Porcine dermal collagen (Permacol) for abdominal wall reconstruction. Curr. Surg. 63, 255–258.
Pascual, G., Sotomayor, S., Rodriguez, M., Perez-Kohler, B., Bellon, J.M., 2012. Repair of abdominal wall defects with biodegradable laminar prostheses: polymeric or biological? PLoS One 7, e52628.
Rohrnbauer, B., Mazza, E., 2013. A non-biological model system to simulate the in vivo mechanical behavior of prosthetic meshes. J. Mech. Behav. Biomed. Mater. 20, 305–315.
Rohrnbauer, B., Mazza, E., 2014. Uniaxial and biaxial mechanical characterization of a prosthetic mesh at different length scales. J. Mech. Behav. Biomed. Mater. 29, 7–19.
Romaniello, F., Mazzaglia, D., Pellegrino, A., Grego, S., Fiorito, R., Ferlosio, A., Chiariello, L., Orlandi, A., 2014. Aortopathy in Marfan syndrome: an update. Cardiovasc. Pathol. 23, 261–266.
Scheidbach, H., Tamme, C., Tannapfel, A., Lippert, H., Kockerling, F., 2004. In vivo studies comparing the biocompatibility of various polypropylene meshes and their handling properties during endoscopic total extraperitoneal (TEP) patchplasty: an experimental study in pigs. Surg. Endosc. 18, 211–220.
Schmidt, C.E., Baier, J.M., 2000. Acellular vascular tissues: natural biomaterials for tissue repair and tissue engineering. Biomaterials 21, 2215–2231.
Sclafani, A.P., Romo 3rd, T., Jacono, A.A., McCormick, S., Cocker, R., Parker, A., 2000.

Evaluation of acellular dermal graft in sheet (AlloDerm) and injectable (micronized AlloDerm) forms for soft tissue augmentation. Clinical observations and histological analysis. Arch. Facial Plast. Surg. 2, 130–136.
Singh, R., Singh, D., Singh, A., 2016. Radiation sterilization of tissue allografts: a review. World J. Radiol. 8, 355–369.
Smart, N., Immanuel, A., Mercer-Jones, M., 2007. Laparoscopic repair of a Littre's hernia with porcine dermal collagen implant (Permacol). Hernia 11, 373–376.
Sungur, N., Uysal, A., Kocer, U., Karaaslan, O., Gumus, M., Sokmensuer, L.K., Sokmensuer, C., 2006. Prevention of tendon adhesions by the reconstruction of the tendon sheath with solvent dehydrated bovine pericard: an experimental study. J. Trauma 61, 1467–1472.
Testini, M., Gurrado, A., Portincasa, P., Scacco, S., Marzullo, A., Piccinni, G., Lissidini, G., Greco, L., De Salvia, M.A., Bonfrate, L., et al., 2014. Bovine pericardium patch wrapping intestinal anastomosis improves healing process and prevents leakage in a pig model. PLoS One 9, e86627.
Todros, S., Pavan, P.G., Pachera, P., Natali, A.N., 2017. Synthetic surgical meshes used in abdominal wall surgery: Part II-Biomechanical aspects. J. Biomed. Mater. Res. B Appl. Biomater. 105, 892–903.
Ueno, T., Pickett, L.C., de la Fuente, S.G., Lawson, D.C., Pappas, T.N., 2004. Clinical application of porcine small intestinal submucosa in the management of infected or potentially contaminated abdominal defects. J. Gastrointest. Surg. 8, 109–112.
Wang, Y., Kim, H.J., Vunjak-Novakovic, G., Kaplan, D.L., 2006. Stem cell-based tissue engineering with silk biomaterials. Biomaterials 27, 6064–6082.
Zheng, M.H., Chen, J., Kirilak, Y., Willers, C., Xu, J., Wood, D., 2005. Porcine small intestine submucosa (SIS) is not an acellular collagenous matrix and contains porcine DNA: possible implications in human implantation. J. Biomed. Mater. Res. B Appl. Biomater. 73, 61–67.
Zonari, A., Novikoff, S., Electo, N.R., Breyner, N.M., Gomes, D.A., Martins, A., Neves, N.M., Reis, R.L., Goes, A.M., 2012. Endothelial differentiation of human stem cells seeded onto electrospun polyhydroxybutyrate/polyhydroxybutyrate-co-hydroxyvalerate fiber mesh. PLoS One 7, e35422.
Zuki, A.B., Hafeez, Y.M., Loqman, M.Y., Noordin, M.M., Norimah, Y., 2007. Effect of preservation methods on the performance of bovine pericardium graft in a rat model. Anat. Histol. Embryol. 36, 349–356.